

## INTERSTELLAR CH<sub>3</sub>CCD

A. J. MARKWICK AND S. B. CHARNLEY

Space Science Division, NASA Ames Research Center, Moffett Field, CA 94035; ajm@ajmarkwick.com, charnley@dusty.arc.nasa.gov

H. M. BUTNER

Joint Astronomy Centre, University Park, Hilo, HI 96720; h.butner@jach.hawaii.edu

AND

T. J. MILLAR

Astrophysics Group, School of Physics and Astronomy, University of Manchester, Sackville Street, Manchester M60 1QD, UK; tom.millar@manchester.ac.uk

Received 2004 June 16; accepted 2005 May 31; published 2005 June 20

### ABSTRACT

We report the detection of a new interstellar molecule: CH<sub>3</sub>CCD, a deuterated isotopomer of methyl acetylene. Analysis of lines detected at seven positions along the ridge of the dark cloud TMC-1 indicates that the CH<sub>3</sub>CCD column density and fractionation exhibit strong spatial gradients, with D/H ratios ranging from a minimum of 0.04 at the cyanopolyne peak (CP) position to as high as 0.18. We find that the column density in CH<sub>2</sub>DCCH is almost constant along the ridge, whereas that of CH<sub>3</sub>CCD increases and that of CH<sub>3</sub>CCH decreases in moving away from the CP. Chemical mechanisms that may explain the observed fractionation trends in CH<sub>3</sub>CCD and CH<sub>2</sub>DCCH are briefly discussed.

*Subject headings:* ISM: abundances — ISM: individual (Taurus Molecular Cloud) — ISM: molecules

### 1. INTRODUCTION

Studies of deuterium chemistry allow us an insight into chemical reaction mechanisms and gas-grain processes, and also may provide us with sensitive probes for the initial phases of protostellar evolution. It is therefore important not only to discover the degree of deuterium fractionation possible in specific interstellar molecules, but also to determine this as a function of environment. Deuterium fractionation can occur at the cold temperatures of dense interstellar clouds through ion-molecule reactions involving deuterated isotopomers of H<sub>3</sub><sup>+</sup> (Millar et al. 2000; Roberts et al. 2003). This chemistry also leads to high atomic D/H ratios and to significant fractionation by atom addition reactions on cold grain surfaces (Tielens 1983). These processes are now understood to be responsible for the extremely high D/H ratios and multiple deuteration recently found in starless cores and around low-mass protostars (e.g., Bacmann et al. 2003; Loinard et al. 2000, 2002; Roueff et al. 2000; van der Tak et al. 2002; Vastel et al. 2003; Parise et al. 2002, 2004). Mapping observations of the dark interstellar cloud TMC-1 have shown spatial abundance gradients to exist in many molecules (see, e.g., Pratap et al. 1997) between the points along the ridge known as the “cyanopolyne peak” and the “ammonia peak” (hereafter CP and AP; see Fig. 1 of Markwick et al. 2001). Attempting to explain the origin of these gradients has been the focus of many theoretical studies (e.g., Hirahara et al. 1992; Suzuki et al. 1992; Markwick et al. 2000). Observations of deuterated species in TMC-1 have also revealed significant spatial gradients in the level of fractionation between these points too, specifically in the molecules HCO<sup>+</sup>, *c*-C<sub>3</sub>H<sub>2</sub>, HC<sub>3</sub>N, HNC, N<sub>2</sub>H<sup>+</sup>, NH<sub>3</sub>, and CH<sub>3</sub>CCH (Guélin et al. 1982; Bell et al. 1988; Howe et al. 1994; Hirota et al. 2001; H. Butner & S. B. Charnley 2005, in preparation; Turner 2001; Markwick et al. 2002, hereafter Paper I).

The first deuterated methyl acetylene isotopomer to be detected was CH<sub>2</sub>DCCH at TMC-1 CP by Gerin et al. (1992, hereafter G92), who also searched unsuccessfully for CH<sub>3</sub>CCD. Prompted by our theoretical work on dynamical-chemical models of deuterium fractionation in TMC-1 (Markwick et al. 2001) and by our existing data for CH<sub>2</sub>DCCH (Paper I), both of which indicated that CH<sub>3</sub>CCD should be present at an observable

abundance, we searched for CH<sub>3</sub>CCD in TMC-1. In this Letter we report the successful detection of interstellar CH<sub>3</sub>CCD at several positions along the TMC-1 ridge.

### 2. OBSERVATIONS AND ANALYSIS

The discovery observations were made between 2002 February 11 and February 26 with the 20 m telescope of the Onsala Space Observatory (OSO). We chose to observe the same lines of CH<sub>3</sub>CCD as searched for by G92, namely, the 6<sub>06</sub>–5<sub>05</sub> A (*K* = 0) and 6<sub>16</sub>–5<sub>15</sub> E (*K* = 1) lines at 93.4560 and 93.4543 GHz, respectively. For consistency, we also reobserved the lines in the main isotopomer. They are the 6<sub>06</sub>–5<sub>05</sub> A and 6<sub>16</sub>–5<sub>15</sub> E lines at 102.548 and 102.546 GHz, respectively. The observations were made with the SIS 100 GHz receiver. The back end was the low-resolution correlator with a bandwidth of 20 MHz and 1600 channels, giving a spectral resolution of 12.5 kHz. The observing mode was dual position beam switching, where the throw was 11'. The pointing errors were typically 2" rms on each axis, determined by observing the IK Tau SiO maser emission. The system temperature was 250 K on average. The beam size of the OSO 20 m at 93 GHz is around 40", and the efficiency at this frequency is 0.6. The data reduction was performed with the XS software provided at the observatory; we averaged the individual scans over position, weighting them according to the system temperature, and removed linear baselines. We then fitted Gaussians to the individual lines to arrive at the integrated intensity.

We also observed TMC-1 in CH<sub>3</sub>CCH, CH<sub>2</sub>DCCH, and CH<sub>3</sub>CCD during a follow-up run with the Kitt Peak 12 m telescope operated by the Arizona Radio Observatory (ARO). The CH<sub>3</sub>CCD and CH<sub>3</sub>CCH lines observed were the same as above, and the CH<sub>2</sub>DCCH line was the 6<sub>06</sub>–5<sub>05</sub> line at 97.081 GHz, as in Paper I. These observations were made between 2003 May 4 and May 15 with the 3 mm receiver. The back-end setup was the 100 kHz filter bank, and the ARO Millimeter Array Correlator was used in 2IF mode to get a spectral resolution of 48.8 kHz. The pointing errors were less than 10" rms on each axis, determined by periodic observation of Saturn or Mars. The system temperature was between 150 and 250 K for all the observations. The beam size of the ARO 12 m at 93 GHz is around 67", and the efficiency is 0.9.

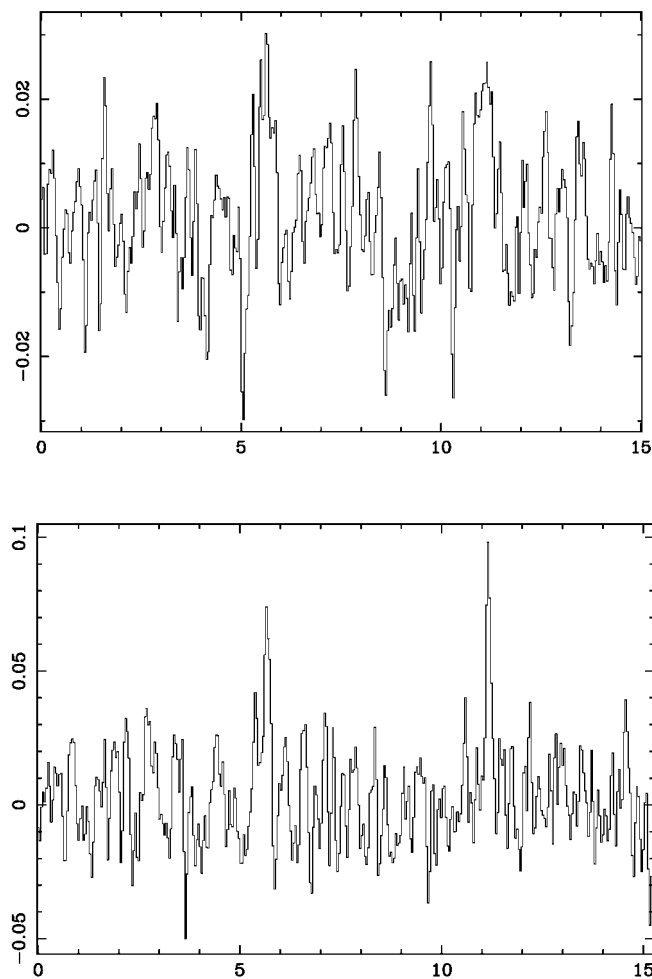


FIG. 1.—Discovery spectra obtained in TMC-1 of  $\text{CH}_3\text{CCD}$  with the OSO 20 m telescope. The top panel is the spectrum at the (0, 0) CP position, while the bottom panel is that at an offset of  $(-160', +240')$ . The ordinates are  $T_{\text{mb}}$  in kelvins and the abscissae are velocity in  $\text{km s}^{-1}$ . The  $K = 1$  line rest frequency is 93.4543 GHz, and TMC-1 is at an LSR velocity of  $5.7 \text{ km s}^{-1}$ .

The data reduction was performed with CLASS, the process being the same as described above for the OSO data.

Figure 1 shows the  $\text{CH}_3\text{CCD}$  discovery spectra made with the OSO 20 m telescope. Figure 2 shows ARO confirming 12 m spectra of  $\text{CH}_3\text{CCD}$  at several positions along the TMC-1 ridge; the lines are all at a common LSR velocity of  $5.7 \text{ km s}^{-1}$ . In these spectra the (0, 0) position is that of the CP: R.A. =  $4^{\text{h}}38^{\text{m}}38^{\text{s}}.0$  and decl. =  $25^{\circ}35'45''.0$  (B1950.0). The  $\text{CH}_3\text{CCD}$  line widths are narrow and similar in magnitude to those of  $\text{CH}_2\text{DCCH}$  and  $\text{CH}_3\text{CCH}$  (G92; Paper I).

The measured intensities and derived column densities from the OSO 20 m and ARO 12 m observations are given in Table 1. Deriving column densities from these observations requires knowledge of the rotational temperature of the molecules. For this, we use the estimates given in Pratap et al. (1997), which were derived from methyl acetylene and which were shown to be consistent with adopting a temperature of 10 K. Since we only observed one line in  $\text{CH}_2\text{DCCH}$ , the  $K = 0$  line, we have assumed that the ortho and para species of  $\text{CH}_2\text{DCCH}$  are of equal abundance, as G92 found. At these low temperatures, the *A* and *E* species of the methyl acetylene isotopomers must be treated separately, and the partition functions are different. We evaluated the partition functions by direct summation using molecular spectroscopic data from the Cologne Database (Müller et al. 2001). The detailed method

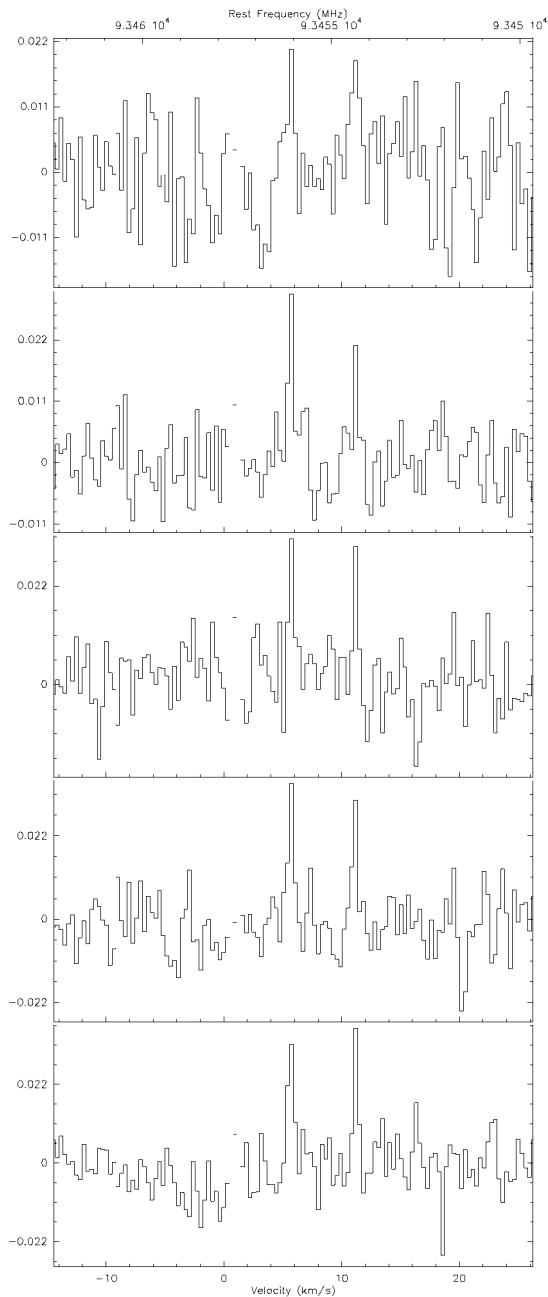


FIG. 2.—Spectra obtained in TMC-1 with the ARO 12 m telescope. The panels are, from top to bottom, the spectra at the offset positions (0, 0) CP,  $(-40', 90')$ ,  $(-80', 150')$ ,  $(-120', 200')$ , and  $(-160', 240')$ . The ordinates are  $T_{\text{mb}}$  in kelvins and the abscissae are velocity in  $\text{km s}^{-1}$ . The  $K = 1$  line rest frequency is 93.4543 GHz, and TMC-1 is at an LSR velocity of  $5.7 \text{ km s}^{-1}$ .

for determining column densities has been given elsewhere (Kuiper et al. 1984; G92; Paper I). The results for all species in all positions are compiled in Table 2, where we list the column densities and the derived ratios in *D/H* and ortho-para spin states. The ortho/para (*A/E*) ratios measured in  $\text{CH}_3\text{CCH}$  and  $\text{CH}_3\text{CCD}$  are around 1 at all the positions. This is the expected value for the transitions we observed.

In total, our observations allowed us to determine the  $\text{CH}_3\text{CCD}/\text{CH}_3\text{CCH}$  ratio at seven positions in TMC-1. We also reobserved the  $\text{CH}_2\text{DCCH}$  and  $\text{CH}_3\text{CCH}$  lines reported in Paper I with the 12 m at four new positions. The fractionation ratios

TABLE 1  
SUMMARY OF INTEGRATED INTENSITIES AND DERIVED COLUMN DENSITIES FOR DETECTED LINES OF CH<sub>3</sub>CCD, CH<sub>2</sub>DCCH, AND CH<sub>3</sub>CCH

OFFSET (arcsec)	LINE	CH <sub>3</sub> CCD <sup>a</sup>		CH <sub>3</sub> CCD <sup>b</sup>		CH <sub>2</sub> DCCH <sup>b</sup>		CH <sub>3</sub> CCH <sup>b</sup>	
		$T_{mb}\Delta v$ (mK km s <sup>-1</sup> )	$N$ (10 <sup>12</sup> cm <sup>-2</sup> )	$T_{R}^*\Delta v$ (mK km s <sup>-1</sup> )	$N$ (10 <sup>12</sup> cm <sup>-2</sup> )	$T_{R}^*\Delta v$ (mK km s <sup>-1</sup> )	$N$ (10 <sup>12</sup> cm <sup>-2</sup> )	$T_{R}^*\Delta v$ (K km s <sup>-1</sup> )	$N$ (10 <sup>12</sup> cm <sup>-2</sup> )
(0, 0)	$K = 0$	9.7 ± 1.3	3.59 ± 0.29	12.26 ± 3.82	3.03 ± 0.85	...	...	0.317*	71.4 ± 4.05
	$K = 1$	11.1 ± 1.4	4.35 ± 0.33	16.15 ± 5.34	4.22 ± 1.26	...	...	0.316*	75.2 ± 4.28
(-40, 90)	$K = 0$	...	...	14.99 ± 2.76	3.70 ± 0.61	47.1	5.57 ± 1.06	0.288	64.8 ± 2.03
	$K = 1$	...	...	8.47 ± 2.78	2.21 ± 0.65	...	...	0.252	60.0 ± 2.14
(-80, 150)	$K = 0$	...	...	14.02 ± 3.70	3.46 ± 0.82	43.1	5.10 ± 1.06	0.283	63.7 ± 2.03
	$K = 1$	...	...	19.37 ± 3.85	5.06 ± 0.91	...	...	0.272	64.7 ± 2.14
(-120, 200)	$K = 0$	...	...	22.23 ± 4.49	5.49 ± 1.00	56.9	6.74 ± 1.06	0.280	63.0 ± 2.03
	$K = 1$	...	...	17.33 ± 3.89	4.53 ± 0.91	...	...	0.286	68.0 ± 2.14
(-160, 240)	$K = 0$	12.6 ± 1.8	5.71 ± 0.76	23.12 ± 3.42	5.15 ± 1.11	72.0*	8.52 ± 2.13	0.209	47.1 ± 2.03
	$K = 1$	15.0 ± 2.0	3.70 ± 0.82	14.18 ± 3.48	4.85 ± 1.18	...	...	0.224	53.3 ± 2.14
(-200, 310)	$K = 0$	15.0 ± 3.3	5.56 ± 0.73	...	...	38.4	4.54 ± 1.06	0.167	37.6 ± 2.03
	$K = 1$	16.7 ± 2.4	6.54 ± 0.56	...	...	...	...	0.194	46.2 ± 2.14
(-280, 420)	$K = 0$	17.2 ± 2.5	6.37 ± 0.56	...	...	...	...	...	...
	$K = 1$	17.1 ± 2.3	6.70 ± 0.54	...	...	...	...	...	...
(-310, 400)	$K = 0$	...	...	...	...	47.3	5.60 ± 1.06	0.179	40.3 ± 2.03
	$K = 1$	...	...	...	...	...	...	0.171	40.7 ± 2.14

NOTES.—The offsets are relative to TMC-1 CP. For CH<sub>2</sub>DCCH and CH<sub>3</sub>CCH the rms errors are not greater than 5 mK km s<sup>-1</sup>, except for entries with an asterisk, for which they are less than twice this value.

<sup>a</sup> Onsala observations.

<sup>b</sup> ARO observations.

are given in Table 2, including some reanalyzed CH<sub>2</sub>DCCH and CH<sub>3</sub>CCH OSO data from Paper I.<sup>1</sup> G92 reported an upper limit of 0.013 for the CH<sub>3</sub>CCD/CH<sub>3</sub>CCH ratio at the TMC-1 CP position, which is not consistent with our observed value of  $0.0395 \pm 0.0024$ .<sup>2</sup>

### 3. DISCUSSION

The derived D/H ratios in the two isotopomers ranges from that typical of many interstellar molecules (~0.04), to values close to some of the highest known (~0.2). Perhaps the most striking result from these observations concerns the relative gradients in column density and D/H ratio between the two isotopomers. Table 2 shows that whereas  $N(\text{CH}_3\text{CCH})$  declines in going from the CP to the AP,  $N(\text{CH}_2\text{DCCH})$  is approximately

<sup>1</sup> The CH<sub>2</sub>DCCH and CH<sub>3</sub>CCH column density gradients are essentially unchanged; the CH<sub>2</sub>DCCH/CH<sub>3</sub>CCH typically agree to within about 70%, the difference due to the corrected treatment of the ortho/para ratio in CH<sub>2</sub>DCCH. At two positions, (0, 0) and (-160, 240), we have observations of the same lines of CH<sub>3</sub>CCD and CH<sub>2</sub>DCCH with both telescopes; in both cases, the observed fractionation ratios agree to within the estimated errors.

<sup>2</sup> Closer inspection reveals that the spectrum of TMC-1 CP published in G92 bears little resemblance to either of our complementary spectra (cf. their Fig. 1 and our Figs. 1 and 2). G92 reported the detection of a  $U$  line at 93.4542 GHz. The line was pronounced in their IRAM 30 m spectrum, having an intensity of 0.06 K. We have independently observed the two lines of CH<sub>3</sub>CCD, but see no sign of the  $U$  line in either the 12 m or OSO spectra. Indeed, it should have been a  $6\sigma$  detection in our Onsala spectrum.

constant and  $N(\text{CH}_3\text{CCD})$  increases. The D/H ratio in each of CH<sub>2</sub>DCCH and CH<sub>3</sub>CCD also increases in a similar manner, but while this characteristic is shared by all molecules in TMC-1 for which D/H ratios have been measured, only part of the increase can be attributed to the fall in  $N(\text{CH}_3\text{CCH})$ .

The origin of these gradients may be explained by considering the formation and fractionation of methyl acetylene. The precursor ion, CH<sub>3</sub>CCH<sub>2</sub><sup>+</sup>, is formed in the ion-molecule reactions



In this scheme, the deuterated ions H<sub>2</sub>D<sup>+</sup> and C<sub>2</sub>HD<sup>+</sup> act to produce only CH<sub>3</sub>CCHD<sup>+</sup>, whereas CH<sub>2</sub>D<sup>+</sup> only forms CH<sub>2</sub>DCCH<sub>2</sub><sup>+</sup>. It is assumed here that deuterons cannot transfer between functional groups (Charnley et al. 1997).

The switching of D atoms into and out of CH<sub>3</sub>CCHD<sup>+</sup> by H<sub>2</sub>D<sup>+</sup> and H<sub>3</sub><sup>+</sup>, with intermediate electron recombinations, dominates the CH<sub>3</sub>CCD chemistry. Hence, the simplest explanation for the  $N(\text{CH}_3\text{CCD})$  gradient, and those of other deuterated

TABLE 2  
MEASURED TOTAL COLUMN DENSITIES, ORTHO/PARA RATIOS, AND DEUTERIUM FRACTIONATION RATIOS ALONG THE TMC-1 RIDGE

Offset (arcsec)	$N(\text{CH}_3\text{CCD})$ (10 <sup>13</sup> cm <sup>-2</sup> )	$N(\text{CH}_2\text{DCCH})$ (10 <sup>13</sup> cm <sup>-2</sup> )	$N(\text{CH}_3\text{CCH})$ (10 <sup>13</sup> cm <sup>-2</sup> )	o-CH <sub>3</sub> CCD		$\frac{\text{CH}_3\text{CCD}}{\text{CH}_3\text{CCH}}$	$\frac{\text{CH}_2\text{DCCH}}{\text{CH}_3\text{CCH}}$	$\frac{\text{CH}_2\text{DCCH}}{\text{CH}_3\text{CCD}}$
				p-CH <sub>3</sub> CCD	p-CH <sub>3</sub> CCH			
(0, 0) <sup>a</sup>	0.79 ± 0.12	1.62 ± 0.22	20.09 ± 2.22	0.72 ± 0.29	0.95 ± 0.08	0.0395 ± 0.007	0.081 ± 0.014	2.04 ± 0.41
(-40, 90)	0.59 ± 0.21	1.11 ± 0.32	12.48 ± 1.08	1.67 ± 0.57	1.08 ± 0.05	0.047 ± 0.018	0.089 ± 0.028	1.88 ± 0.86
(-80, 150)	0.85 ± 0.27	1.02 ± 0.32	12.84 ± 1.41	0.68 ± 0.20	0.98 ± 0.05	0.066 ± 0.022	0.079 ± 0.026	1.20 ± 0.53
(-120, 200)	1.00 ± 0.29	1.35 ± 0.33	13.11 ± 1.44	1.21 ± 0.33	0.93 ± 0.04	0.076 ± 0.024	0.103 ± 0.028	1.34 ± 0.51
(-160, 240)	0.94 ± 0.26	1.70 ± 0.63	10.03 ± 1.16	1.54 ± 0.40	0.88 ± 0.05	0.094 ± 0.028	0.170 ± 0.065	1.81 ± 0.83
(-200, 310)	1.21 ± 0.23 <sup>a</sup>	0.91 ± 0.31	8.38 ± 1.03	0.85 ± 0.13 <sup>a</sup>	1.51 ± 0.13 <sup>a</sup>	0.175 ± 0.040 <sup>a</sup>	0.108 ± 0.040	0.75 ± 0.40 <sup>b</sup>
(-280, 420)	1.31 ± 0.20 <sup>a</sup>	...	7.26 ± 0.96 <sup>a</sup>	0.95 ± 0.11 <sup>a</sup>	1.26 ± 0.11 <sup>a</sup>	0.180 ± 0.037 <sup>a</sup>	...	...
(-310, 400)	...	1.12 ± 0.32	8.10 ± 1.00	...	0.99 ± 0.072	...	0.138 ± 0.043	...

NOTE.—We added an additional error term of 10% to the column density determinations, to account for the absolute calibration and tuning errors of the telescope.

<sup>a</sup> Onsala observational data.

<sup>b</sup> Number derived from OSO and ARO data.

molecules listed in § 1, is that there is a gradient in the  $\text{H}_2\text{D}^+/\text{H}_3^+$  ratio, with the lower values near the CP. Enhancement of  $\text{H}_2\text{D}^+$  by depletion of CO onto grains (e.g., Roberts & Millar 2000) is possible. The alternative is a purely gas-phase explanation involving  $\text{H}_2\text{D}^+$  depletion. It has been proposed that ion-neutral streaming (ambipolar diffusion) induced by magnetohydrodynamic waves is occurring along the TMC-1 ridge (Markwick et al. 2000) at relative velocities sufficient to drive only  $\text{H}_2\text{D}^+$  removal in endoergic reactions with  $\text{H}_2$  (Charnley 1998). The physical origin of this ambipolar diffusion gradient in TMC-1 could be either MHD waves generated by the class 0 protostar IRAS 04381+2540, relative clump motions, or turbulence (Markwick et al. 2000; Dickens et al. 2001). The constancy along the ridge of  $N(\text{CH}_2\text{DCCH})$  and, within the errors, shallower  $N(\text{CH}_2\text{DCCH})/N(\text{CH}_3\text{CCH})$  gradient can then be understood as due to two chemical processes. Due to the higher endoergicity of its reaction with  $\text{H}_2$ ,  $\text{CH}_2\text{D}^+$  is unaffected by such low-amplitude waves and so would still produce  $\text{CH}_2\text{D}$ , all along the ridge, in the reaction analogous to reaction (2) above. Furthermore, regions with higher gas-phase  $\text{H}_2\text{D}^+$  abundances will be able to feed D more efficiently into a simple hydrocarbon chemistry, and this will lead to higher  $\text{CH}_3\text{D}/\text{CH}_4$  ratios approaching the AP, and hence to enhanced  $\text{CH}_2\text{DCCH}_2^+$  production there via the analog of reaction (3) above.

Ambipolar diffusion would also explain generally why the ratio  $R (= \text{CH}_2\text{DCCH}/\text{CH}_3\text{CCD})$  appears to be higher at the CP. Based on this deuteration chemistry, with each point of the TMC-1 ridge being affected by the propagation of MHD waves at some point in its past, Markwick et al. (2001) presented an evolutionary model that predicted  $R = 2.5$  at the CP position. This is only marginally consistent with our observed value of  $2.04 \pm 0.41$ . One important uncertainty when making quantitative comparisons with models of deuterium chemistry like that of Markwick et al. (2001) is that in the absence of experimental evidence to the contrary, electron recombination product branching ratios are assumed to be statistical. Results for other deuterated ions  $\text{HD}_2\text{O}^+$ ,  $\text{H}_2\text{D}^+$ , and  $\text{ND}_3\text{H}^+$  (Gellene & Porter 1984; Larsson et al. 1996; Jensen et al. 2000) indicate that deuterium may be selectively retained following dissoci-

ative recombination; this may also be the case for  $\text{CH}_3\text{CCHD}^+$ , and so  $R$  will be sensitive to this uncertainty. For example, if we assume that recombination of  $\text{CH}_3\text{CCHD}^+$  produces  $\text{CH}_3\text{CCD}$  three times as often as it produces  $\text{CH}_3\text{CCH}$ , i.e., that the ratio of H to D atom loss is 3 : 1 instead of 1 : 1, then  $R = 2$ . Nevertheless, although  $R$  varies with position, changing the branching ratio in this way would reduce it uniformly along the ridge, and so this model could still account for the deuterium fractionation gradient observed in  $\text{CH}_3\text{CCD}$  and  $\text{CH}_2\text{DCCH}$ .

#### 4. CONCLUSIONS

We have made the first detection of  $\text{CH}_3\text{CCD}$  in space. The measured  $\text{CH}_3\text{CCD}/\text{CH}_3\text{CCH}$  ratio at several positions along the TMC-1 ridge varies from modest ( $\sim 0.04$ ) to high values ( $\sim 0.18$ ). We have also determined that the column densities of each of  $\text{CH}_3\text{CCD}$ ,  $\text{CH}_3\text{CCH}$ , and  $\text{CH}_2\text{DCCH}$  have significantly different spatial gradients in TMC-1. These and the associated D/H gradients can be understood in the context of a model where  $\text{H}_2\text{D}^+$  is destroyed nonthermally in chemical reactions, probably driven by ion-neutral streaming in MHD motions. The high D/H ratios observed lead us to expect that other deuterated isotopomers of methyl acetylene are present in TMC-1:  $\text{CD}_2\text{HCCH}$ ,  $\text{CH}_2\text{DCCD}$ ,  $\text{CD}_3\text{CCH}$ ,  $\text{CD}_2\text{HCCD}$ , and  $\text{CD}_3\text{CCD}$ ; future studies of these molecules could provide important information on deuterium fractionation pathways in dark clouds.

This work was supported by NASA's Origins of Solar Systems and Exobiology Programs through NASA Ames cooperative agreement NCC2-1412 with the SETI Institute. A. J. M. is supported by an NRC Resident Research Associateship. Research in Astrophysics at UMIST is supported by PPARC. We acknowledge M. Gerin for pointing out an error in the data reduction of Paper I, and H. Müller for discussion of the spin statistics and partition functions of deuterated isotopomers of  $\text{CH}_3\text{CCH}$ . A. J. M. is grateful to the staff of the Onsala Space Observatory, and in particular to Lars E. B. Johansson and Per Bergman, for their continuing support during observing runs.

#### REFERENCES

- Bacmann, A., Lefloch, B., Ceccarelli, C., Steinacker, J., Castets, A., & Loinard, L. 2003, *ApJ*, 585, L55
- Bell, M. B., et al. 1988, *ApJ*, 326, 924
- Charnley, S. B. 1998, *MNRAS*, 298, L25
- Charnley, S. B., Tielens, A. G. G. M., & Rodgers, S. D. 1997, *ApJ*, 482, L203
- Dickens, J. E., Langer, W. D., & Velusamy, T. 2001, *ApJ*, 558, 693
- Gellene, G. I., & Porter, R. F. 1984, *J. Phys. Chem.*, 88, 6680
- Gerin, M., Combes, F., Wlodarczak, G., Encrenaz, P., & Laurent, C. 1992, *A&A*, 253, L29 (G92)
- Guélin, M., Langer, W. D., & Wilson, R. W. 1982, *A&A*, 107, 107
- Hirahara, Y., et al. 1992, *ApJ*, 394, 539
- Hirota, T., Ikeda, M., & Yamamoto, S. 2001, *ApJ*, 547, 814
- Howe, D. A., Millar, T. J., Schilke, P., & Walmsley, C. M. 1994, *MNRAS*, 267, 59
- Jensen, M. J., Bilodeau, R. C., Safvan, C. P., Seiersen, K., & Andersen, L. H. 2000, *ApJ*, 543, 764
- Kuiper, T. B. H., Kuiper, E. N. R., Dickinson, D. F., Turner, B. E., & Zuckerman, B. 1984, *ApJ*, 276, 211
- Larsson, M., et al. 1996, *A&A*, 309, L1
- Loinard, L., Castets, A., Ceccarelli, C., Tielens, A. G. G. M., Faure, A., Caux, E., & Duvert, G. 2000, *A&A*, 359, 1169
- Loinard, L., et al. 2002, *Planet. Space Sci.*, 50, 1205
- Markwick, A. J., Charnley, S. B., & Millar, T. J. 2001, *A&A*, 376, 1054
- Markwick, A. J., Millar, T. J., & Charnley, S. B. 2000, *ApJ*, 535, 256
- . 2002, *A&A*, 381, 560 (Paper I)
- Millar, T. J., Roberts, H., Markwick, A. J., & Charnley, S. B. 2000, *Philos. Trans. R. Soc. London A*, 358, 2535
- Müller, H. S. P., Thorwirth, S., Roth, D. A., & Winnewisser, G. 2001, *A&A*, 370, L49
- Parise, B., Castets, A., Herbst, E., Caux, E., Ceccarelli, C., Mukhopadhyay, I., & Tielens, A. G. G. M. 2004, *A&A*, 416, 159
- Parise, B., et al. 2002, *A&A*, 393, L49
- Pratap, P., Dickens, J. E., Snell, R. L., Miralles, M. P., Bergin, E. A., Irvine, W. M., & Schloerb, F. P. 1997, *ApJ*, 486, 862
- Roberts, H., Herbst, E., & Millar, T. J. 2003, *ApJ*, 591, L41
- Roberts, H., & Millar, T. J. 2000, *A&A*, 361, 388
- Roueff, E., Tiné, S., Coudert, L. H., Pineau des Forêts, G., Falgarone, E., & Gerin, M. 2000, *A&A*, 354, L63
- Suzuki, H., et al. 1992, *ApJ*, 392, 551
- Tielens, A. G. G. M. 1983, *A&A*, 119, 177
- Turner, B. E. 2001, *ApJS*, 136, 579
- van der Tak, F. F. S., Schilke, P., Müller, H. S. P., Lis, D. C., Phillips, T. G., Gerin, M., & Roueff, E. 2002, *A&A*, 388, L53
- Vastel, C., Phillips, T. G., Ceccarelli, C., & Pearson, J. 2003, *ApJ*, 593, L97